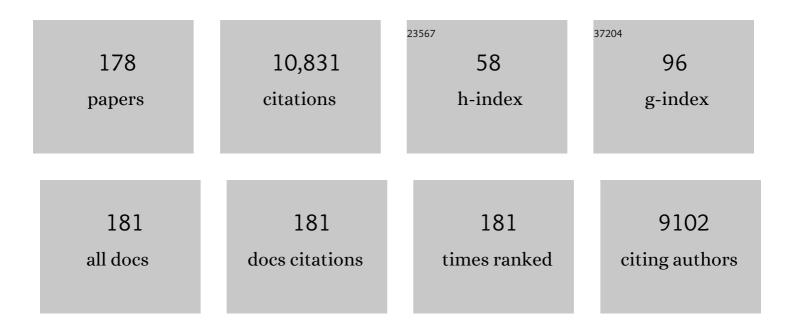
Zhao-Yang Li

List of Publications by Year in descending order

Source: https://exaly.com/author-pdf/2116262/publications.pdf Version: 2024-02-01



#	Article	IF	CITATIONS
1	Flower-like CuS/graphene oxide with photothermal and enhanced photocatalytic effect for rapid bacteria-killing using visible light. Rare Metals, 2022, 41, 639-649.	7.1	61
2	3D N-doped mesoporous carbon/SnO2 with polypyrrole coating layer as high-performance anode material for Li-ion batteries. Journal of Alloys and Compounds, 2022, 892, 162083.	5.5	20
3	Amorphous FeNiNbPC nanoprous structure for efficient and stable electrochemical oxygen evolution. Journal of Colloid and Interface Science, 2022, 608, 1973-1982.	9.4	13
4	Theory-screened MOF-based single-atom catalysts for facile and effective therapy of biofilm-induced periodontitis. Chemical Engineering Journal, 2022, 431, 133279.	12.7	31
5	The enhanced photocatalytic sterilization of MOF-Based nanohybrid for rapid and portable therapy of bacteria-infected open wounds. Bioactive Materials, 2022, 13, 200-211.	15.6	47
6	Oxygen Vacanciesâ€Rich Heterojunction of Ti ₃ C ₂ /BiOBr for Photoâ€Excited Antibacterial Textiles. Small, 2022, 18, e2104448.	10.0	31
7	Using tea nanoclusters as β-lactamase inhibitors to cure multidrug-resistant bacterial pneumonia: A promising therapeutic strategy by Chinese materioherbology. Fundamental Research, 2022, 2, 496-504.	3.3	11
8	A soft intelligent dressing with pH and temperature sensors for early detection of wound infection. RSC Advances, 2022, 12, 3243-3252.	3.6	7
9	Optimizing the strontium content to achieve an ideal osseointegration through balancing apatite-forming ability and osteogenic activity. Materials Science and Engineering C, 2022, 133, 112647.	7.3	21
10	Photo-excited antibacterial poly(ƕcaprolactone)@MoS2/ZnS hybrid nanofibers. Chemical Engineering Journal, 2022, 434, 134764.	12.7	13
11	Automatic phantom-less QCT system with high precision of BMD measurement for osteoporosis screening: Technique optimisation and clinical validation. Journal of Orthopaedic Translation, 2022, 33, 24-30.	3.9	12
12	Noble metal-based nanomaterials as antibacterial agents. Journal of Alloys and Compounds, 2022, 904, 164091.	5.5	56
13	Gelatin/gentamicin sulfate-modified PMMA bone cement with proper mechanical properties and high antibacterial ability. Materials Research Express, 2022, 9, 035405.	1.6	6
14	Simulation and Prediction of the Impact of Climate Change Scenarios on Runoff of Typical Watersheds in Changbai Mountains, China. Water (Switzerland), 2022, 14, 792.	2.7	8
15	Self-standing nanoporous NiPd bimetallic electrocatalysts with ultra-low Pd loading for efficient hydrogen evolution reaction. Electrochimica Acta, 2022, 411, 140077.	5.2	15
16	Recent progress of photo-excited antibacterial materials via chemical vapor deposition. Chemical Engineering Journal, 2022, 437, 135401.	12.7	15
17	Surface photodynamic ion sterilization of ITO-Cu2O/ZnO preventing touch infection. Journal of Materials Science and Technology, 2022, 122, 10-19.	10.7	10
18	Simultaneously enhancing the photocatalytic and photothermal effect of NH2-MIL-125-GO-Pt ternary heterojunction for rapid therapy of bacteria-infected wounds. Bioactive Materials, 2022, 18, 421-432.	15.6	42

#	Article	IF	CITATIONS
19	High-performance five-ring-fused organic semiconductors for field-effect transistors. Chemical Society Reviews, 2022, 51, 3071-3122.	38.1	49
20	Nanoporous Ni/NiO catalyst for efficient hydrogen evolution reaction prepared by partial electro-oxidation after dealloying. Journal of Alloys and Compounds, 2022, 911, 165061.	5.5	16
21	Electrodeposition of self-supported NiMo amorphous coating as an efficient and stable catalyst for hydrogen evolution reaction. Rare Metals, 2022, 41, 2624-2632.	7.1	29
22	Analysis of Landscape Change and Its Driving Mechanism in Chagan Lake National Nature Reserve. Sustainability, 2022, 14, 5675.	3.2	3
23	A Three-Dimensional Cement Quantification Method for Decision Prediction of Vertebral Recompression after Vertebroplasty. Computational and Mathematical Methods in Medicine, 2022, 2022, 1-14.	1.3	1
24	Microwave assisted antibacterial action of Garcinia nanoparticles on Gram-negative bacteria. Nature Communications, 2022, 13, 2461.	12.8	49
25	A smart strategy of "laser-direct-writing―to achieve scalable fabrication of self-supported MoNi ₄ /Ni catalysts for efficient and durable hydrogen evolution reaction. Journal of Materials Chemistry A, 2022, 10, 12722-12732.	10.3	8
26	Optimal Planning and Management of Land Use in River Source Region: A Case Study of Songhua River Basin, China. International Journal of Environmental Research and Public Health, 2022, 19, 6610.	2.6	5
27	Interface Polarization Strengthened Microwave Catalysis of MoS ₂ /FeS/Rhein for the Therapy of Bacteriaâ€Infected Osteomyelitis. Advanced Functional Materials, 2022, 32, .	14.9	26
28	Atomic-layer Fe2O3-modified 2D porphyrinic metal-organic framework for enhanced photocatalytic disinfection through electron-withdrawing effect. Applied Catalysis B: Environmental, 2022, 317, 121701.	20.2	22
29	Zr55Al10Ni5Cu30 amorphous alloy film prepared by magnetron sputtering method. Rare Metals, 2021, 40, 2237-2243.	7.1	6
30	Eco-friendly and degradable red phosphorus nanoparticles for rapid microbial sterilization under visible light. Journal of Materials Science and Technology, 2021, 67, 70-79.	10.7	31
31	Photothermy-strengthened photocatalytic activity of polydopamine-modified metal-organic frameworks for rapid therapy of bacteria-infected wounds. Journal of Materials Science and Technology, 2021, 62, 83-95.	10.7	91
32	Photo-controlled degradation of PLGA/Ti3C2 hybrid coating on Mg-Sr alloy using near infrared light. Bioactive Materials, 2021, 6, 568-578.	15.6	30
33	Nano-needle strontium-substituted apatite coating enhances osteoporotic osseointegration through promoting osteogenesis and inhibiting osteoclastogenesis. Bioactive Materials, 2021, 6, 905-915.	15.6	51
34	In situ synthesis of a novel Mn3O4/g-C3N4 p-n heterostructure photocatalyst for water splitting. Journal of Colloid and Interface Science, 2021, 586, 778-784.	9.4	52
35	Self-supported Ni3Se2@NiFe layered double hydroxide bifunctional electrocatalyst for overall water splitting. Journal of Colloid and Interface Science, 2021, 587, 79-89.	9.4	89
36	A novel snail-inspired bionic design of titanium with strontium-substituted hydroxyapatite coating for promoting osseointegration. Journal of Materials Science and Technology, 2021, 79, 35-45.	10.7	27

#	Article	IF	CITATIONS
37	Ag3PO4 decorated black urchin-like defective TiO2 for rapid and long-term bacteria-killing under visible light. Bioactive Materials, 2021, 6, 1575-1587.	15.6	85
38	Highly durable Cu–N–C active sites towards efficient oxygen reduction for zinc-air battery: Carbon matrix effect, reaction mechanism and pathways. Journal of Alloys and Compounds, 2021, 857, 158321.	5.5	12
39	Ultrasonic Interfacial Engineering of Red Phosphorous–Metal for Eradicating MRSA Infection Effectively. Advanced Materials, 2021, 33, e2006047.	21.0	93
40	Structure engineering of electrodeposited NiMoÂfilms for highly efficient and durable seawater splitting. Electrochimica Acta, 2021, 365, 137366.	5.2	45
41	Antibacterial Hybrid Hydrogels. Macromolecular Bioscience, 2021, 21, e2000252.	4.1	105
42	Recent Progress in Photocatalytic Antibacterial. ACS Applied Bio Materials, 2021, 4, 3909-3936.	4.6	100
43	The recent progress on metal–organic frameworks for phototherapy. Chemical Society Reviews, 2021, 50, 5086-5125.	38.1	262
44	Study on Environmental Factors of Fluorine in Chagan Lake Catchment, Northeast China. Water (Switzerland), 2021, 13, 629.	2.7	7
45	Photothermal-controlled sustainable degradation of protective coating modified Mg alloy using near-infrared light. Rare Metals, 2021, 40, 2538-2551.	7.1	14
46	Interfacial engineering of Bi2S3/Ti3C2Tx MXene based on work function for rapid photo-excited bacteria-killing. Nature Communications, 2021, 12, 1224.	12.8	283
47	Highly efficient nanoporous CoBP electrocatalyst for hydrogen evolution reaction. Rare Metals, 2021, 40, 1031-1039.	7.1	42
48	Boosting oxygen reduction catalysis with abundant single atom tin active sites in zinc-air battery. Journal of Power Sources, 2021, 490, 229483.	7.8	19
49	Unveiling the roles of multiple active sites during oxygen reduction reaction in Cr2O3@Cr-N-C composite catalyst. Journal of Catalysis, 2021, 396, 402-408.	6.2	9
50	Spin State Tuning of the Octahedral Sites in Ni–Co-Based Spinel toward Highly Efficient Urea Oxidation Reaction. Journal of Physical Chemistry C, 2021, 125, 9190-9199.	3.1	25
51	Na+ inserted metal-organic framework for rapid therapy of bacteria-infected osteomyelitis through microwave strengthened Fenton reaction and thermal effects. Nano Today, 2021, 37, 101090.	11.9	77
52	Single-Atom Catalysis for Efficient Sonodynamic Therapy of Methicillin-Resistant <i>Staphylococcus aureus</i> -Infected Osteomyelitis. ACS Nano, 2021, 15, 10628-10639.	14.6	144
53	Influences of strontium on the phase composition and lattice structure of biphasic calcium phosphate. Ceramics International, 2021, 47, 16248-16255.	4.8	10
54	Nanoporous Nickel–Molybdenum Oxide with an Oxygen Vacancy for Electrocatalytic Nitrogen Fixation under Ambient Conditions. ACS Applied Materials & Interfaces, 2021, 13, 30722-30730.	8.0	34

#	Article	IF	CITATIONS
55	ZIF-67 derived Co@NC/g-C3N4 as a photocatalyst for enhanced water splitting H2 evolution. Environmental Research, 2021, 197, 111002.	7.5	21
56	Enhanced Electrocatalysis for Hydrogen Evolution over a Nanoporous NiAlTi/Al ₃ Ti Hybrid. ACS Applied Energy Materials, 2021, 4, 7579-7588.	5.1	6
57	An Engineered Pseudoâ€Macrophage for Rapid Treatment of Bacteriaâ€Infected Osteomyelitis via Microwaveâ€Excited Antiâ€Infection and Immunoregulation. Advanced Materials, 2021, 33, e2102926.	21.0	87
58	2D MOF Periodontitis Photodynamic Ion Therapy. Journal of the American Chemical Society, 2021, 143, 15427-15439.	13.7	161
59	Sandwich structured Ni3S2-MoS2-Ni3S2@Ni foam electrode as a stable bifunctional electrocatalyst for highly sustained overall seawater splitting. Electrochimica Acta, 2021, 390, 138833.	5.2	41
60	Electronic Structure Modulation of Nanoporous Cobalt Phosphide by Carbon Doping for Alkaline Hydrogen Evolution Reaction. Advanced Functional Materials, 2021, 31, 2107333.	14.9	104
61	The enhanced near-infrared photocatalytic and photothermal effects of MXene-based heterojunction for rapid bacteria-killing. Applied Catalysis B: Environmental, 2021, 297, 120500.	20.2	68
62	A self-supported FeNi layered double hydroxide anode with high activity and long-term stability for efficient oxygen evolution reaction. Sustainable Energy and Fuels, 2021, 5, 3205-3212.	4.9	3
63	Ni ₂ P nanoflakes for the high-performing urea oxidation reaction: linking active sites to a UOR mechanism. Nanoscale, 2021, 13, 1759-1769.	5.6	106
64	Photo-Sono Interfacial Engineering Exciting the Intrinsic Property of Herbal Nanomedicine for Rapid Broad-Spectrum Bacteria Killing. ACS Nano, 2021, 15, 18505-18519.	14.6	61
65	Self-activating anti-infection implant. Nature Communications, 2021, 12, 6907.	12.8	77
66	Near-infrared light controlled fast self-healing protective coating on magnesium alloy. Corrosion Science, 2020, 163, 108257.	6.6	55
67	Photo-responsive chitosan/Ag/MoS2 for rapid bacteria-killing. Journal of Hazardous Materials, 2020, 383, 121122.	12.4	153
68	An UV to NIR-driven platform based on red phosphorus/graphene oxide film for rapid microbial inactivation. Chemical Engineering Journal, 2020, 383, 123088.	12.7	52
69	Enhanced photocatalytic activity and photothermal effects of cu-doped metal-organic frameworks for rapid treatment of bacteria-infected wounds. Applied Catalysis B: Environmental, 2020, 261, 118248.	20.2	255
70	Modulation of the mechanosensing of mesenchymal stem cells by laser-induced patterning for the acceleration of tissue reconstruction through the Wnt/β-catenin signaling pathway activation. Acta Biomaterialia, 2020, 101, 152-167.	8.3	51
71	Preparation and physicochemical properties of an injectable alginate-based hydrogel by the regulated release of divalent ions via the hydrolysis of <scp>d</scp> -glucono- δ -lactone. Journal of Biomaterials Applications, 2020, 34, 891-901.	2.4	6
72	Zn2+-assisted photothermal therapy for rapid bacteria-killing using biodegradable humic acid encapsulated MOFs. Colloids and Surfaces B: Biointerfaces, 2020, 188, 110781.	5.0	41

#	Article	IF	CITATIONS
73	Eco-friendly Hybrids of Carbon Quantum Dots Modified MoS ₂ for Rapid Microbial Inactivation by Strengthened Photocatalysis. ACS Sustainable Chemistry and Engineering, 2020, 8, 534-542.	6.7	53
74	Tuning the π-electron delocalization degree of mesoporous carbon for hydrogen peroxide electrochemical generation. Journal of Catalysis, 2020, 392, 1-7.	6.2	10
75	Rutile-Coated B-Phase TiO ₂ Heterojunction Nanobelts for Photocatalytic H ₂ Evolution. ACS Applied Nano Materials, 2020, 3, 10349-10359.	5.0	18
76	Photoresponsive Materials for Antibacterial Applications. Cell Reports Physical Science, 2020, 1, 100245.	5.6	102
77	Novel Bionic Topography with MiR-21 Coating for Improving Bone-Implant Integration through Regulating Cell Adhesion and Angiogenesis. Nano Letters, 2020, 20, 7716-7721.	9.1	41
78	Treatment of MRSA-infected osteomyelitis using bacterial capturing, magnetically targeted composites with microwave-assisted bacterial killing. Nature Communications, 2020, 11, 4446.	12.8	165
79	Amorphous CoMoO ₄ with Nanoporous Structures for Electrochemical Ammonia Synthesis under Ambient Conditions. ACS Sustainable Chemistry and Engineering, 2020, 8, 19072-19083.	6.7	15
80	Relationships between Temporal and Spatial Changes in Lakes and Climate Change in the Saline-Alkali Concentrated Distribution Area in the Southwest of Songnen Plain, Northeast China, from 1985 to 2015. Water (Switzerland), 2020, 12, 3557.	2.7	5
81	Cicada-inspired fluoridated hydroxyapatite nanostructured surfaces synthesized by electrochemical additive manufacturing. Materials and Design, 2020, 193, 108790.	7.0	36
82	UV-irradiation induced biological activity and antibacterial activity of ZnO coated magnesium alloy. Materials Science and Engineering C, 2020, 114, 110997.	7.3	19
83	Controllable phase transformation of fluoridated calcium phosphate ultrathin coatings for biomedical applications. Journal of Alloys and Compounds, 2020, 847, 155920.	5.5	10
84	The rapid photoresponsive bacteria-killing of Cu-doped MoS ₂ . Biomaterials Science, 2020, 8, 4216-4224.	5.4	57
85	Overcoming Multidrugâ€Resistant MRSA Using Conventional Aminoglycoside Antibiotics. Advanced Science, 2020, 7, 1902070.	11.2	49
86	miR-21 promotes osseointegration and mineralization through enhancing both osteogenic and osteoclastic expression. Materials Science and Engineering C, 2020, 111, 110785.	7.3	25
87	Near-Infrared Light Triggered Phototherapy and Immunotherapy for Elimination of Methicillin-Resistant <i>Staphylococcus aureus</i> Biofilm Infection on Bone Implant. ACS Nano, 2020, 14, 8157-8170.	14.6	133
88	Ce and Er Co-doped TiO2 for rapid bacteria- killing using visible light. Bioactive Materials, 2020, 5, 201-209.	15.6	61
89	Visible light responsive CuS/ protonated g-C3N4 heterostructure for rapid sterilization. Journal of Hazardous Materials, 2020, 393, 122423.	12.4	116
90	In-situ sulfuration of Cu-based metal-organic framework for rapid near-infrared light sterilization. Journal of Hazardous Materials, 2020, 390, 122126.	12.4	72

#	Article	IF	CITATIONS
91	Rapid Photo-Sonotherapy for Clinical Treatment of Bacterial Infected Bone Implants by Creating Oxygen Deficiency Using Sulfur Doping. ACS Nano, 2020, 14, 2077-2089.	14.6	182
92	Rapid Sterilization by Photocatalytic Ag ₃ PO ₄ /α-Fe ₂ O ₃ Composites Using Visible Light. ACS Sustainable Chemistry and Engineering, 2020, 8, 2577-2585.	6.7	53
93	Engineered probiotics biofilm enhances osseointegration via immunoregulation and anti-infection. Science Advances, 2020, 6, .	10.3	82
94	Strontium Doped Hydroxyapatite Nanoparticles: Synthesis, Characterization and Simulation. Wuji Cailiao Xuebao/Journal of Inorganic Materials, 2020, , 439.	1.3	0
95	Identifying compositional and structural changes in the nucleus pulposus from patients with lumbar disc herniation using Raman spectroscopy. Experimental and Therapeutic Medicine, 2020, 20, 447-453.	1.8	4
96	Synthesis of polyaluminocarbosilane with low branched molecular structure using liquid polysilacarbosilane and aluminum acetylacetonate by highâ€pressure method. Applied Organometallic Chemistry, 2019, 33, e4720.	3.5	6
97	Strontium inhibits osteoclastogenesis by enhancing LRP6 and β-catenin-mediated OPG targeted by miR-181d-5p. Journal of Cell Communication and Signaling, 2019, 13, 85-97.	3.4	11
98	Lysozyme-Assisted Photothermal Eradication of Methicillin-Resistant <i>Staphylococcus aureus</i> Infection and Accelerated Tissue Repair with Natural Melanosome Nanostructures. ACS Nano, 2019, 13, 11153-11167.	14.6	74
99	Dual Metal–Organic Framework Heterointerface. ACS Central Science, 2019, 5, 1591-1601.	11.3	108
100	Ag ₂ S@WS ₂ Heterostructure for Rapid Bacteria-Killing Using Near-Infrared Light. ACS Sustainable Chemistry and Engineering, 2019, 7, 14982-14990.	6.7	67
101	A near infrared-activated photocatalyst based on elemental phosphorus by chemical vapor deposition. Applied Catalysis B: Environmental, 2019, 258, 117980.	20.2	30
102	Highly Effective and Noninvasive Nearâ€Infrared Eradication of a <i>Staphylococcus aureus</i> Biofilm on Implants by a Photoresponsive Coating within 20 Min. Advanced Science, 2019, 6, 1900599.	11.2	212
103	Superimposed surface plasma resonance effect enhanced the near-infrared photocatalytic activity of Au@Bi2WO6 coating for rapid bacterial killing. Journal of Hazardous Materials, 2019, 380, 120818.	12.4	85
104	Highly Efficient and Self-Standing Nanoporous NiO/Al ₃ Ni ₂ Electrocatalyst for Hydrogen Evolution Reaction. ACS Applied Energy Materials, 2019, 2, 7913-7922.	5.1	38
105	Photoelectric-Responsive Extracellular Matrix for Bone Engineering. ACS Nano, 2019, 13, 13581-13594.	14.6	51
106	Ag2S decorated nanocubes with enhanced near-infrared photothermal and photodynamic properties for rapid sterilization. Colloids and Interface Science Communications, 2019, 33, 100201.	4.1	44
107	Rapid Biofilm Elimination on Bone Implants Using Nearâ€Infraredâ€Activated Inorganic Semiconductor Heterostructures. Advanced Healthcare Materials, 2019, 8, e1900835.	7.6	71
108	AgBr Nanoparticles in Situ Growth on 2D MoS ₂ Nanosheets for Rapid Bacteria-Killing and Photodisinfection. ACS Applied Materials & Interfaces, 2019, 11, 34364-34375.	8.0	58

#	Article	IF	CITATIONS
109	Zinc-doped Prussian blue enhances photothermal clearance of Staphylococcus aureus and promotes tissue repair in infected wounds. Nature Communications, 2019, 10, 4490.	12.8	306
110	Enhancement of photocatalytic H2 production by metal complex electrostatic adsorption on TiO2 (B) nanosheets. Journal of Materials Chemistry A, 2019, 7, 3797-3804.	10.3	11
111	Enhancing the antibacterial efficacy of low-dose gentamicin with 5 minute assistance of photothermy at 50 ŰC. Biomaterials Science, 2019, 7, 1437-1447.	5.4	56
112	Strontium promotes osteogenic differentiation by activating autophagy via the the AMPK/mTOR signaling pathway in MC3T3‑E1 cells. International Journal of Molecular Medicine, 2019, 44, 652-660.	4.0	34
113	Self-supported Ni(OH)2/MnO2 on CFP as a flexible anode towards electrocatalytic urea conversion: The role of composition on activity, redox states and reaction dynamics. Electrochimica Acta, 2019, 318, 32-41.	5.2	33
114	Surfactant-free electrochemical synthesis of fluoridated hydroxyapatite nanorods for biomedical applications. Ceramics International, 2019, 45, 17336-17343.	4.8	9
115	The enhanced photocatalytic properties of MnO2/g-C3N4 heterostructure for rapid sterilization under visible light. Journal of Hazardous Materials, 2019, 377, 227-236.	12.4	122
116	Precisely Controlled Delivery of Abaloparatide through Injectable Hydrogel to Promote Bone Regeneration. Macromolecular Bioscience, 2019, 19, e1900020.	4.1	28
117	Local Photothermal/Photodynamic Synergistic Therapy by Disrupting Bacterial Membrane To Accelerate Reactive Oxygen Species Permeation and Protein Leakage. ACS Applied Materials & Interfaces, 2019, 11, 17902-17914.	8.0	149
118	Rapid and Superior Bacteria Killing of Carbon Quantum Dots/ZnO Decorated Injectable Folic Acid onjugated PDA Hydrogel through Dual‣ight Triggered ROS and Membrane Permeability. Small, 2019, 15, e1900322.	10.0	180
119	Eradicating Multidrugâ€Resistant Bacteria Rapidly Using a Multi Functional gâ€C ₃ N ₄ @ Bi ₂ S ₃ Nanorod Heterojunction with or without Antibiotics. Advanced Functional Materials, 2019, 29, 1900946.	14.9	136
120	Photocatalysis: Lightâ€Activated Rapid Disinfection by Accelerated Charge Transfer in Red Phosphorus/ZnO Heterointerface (Small Methods 3/2019). Small Methods, 2019, 3, 1970008.	8.6	4
121	Rapid and Highly Effective Noninvasive Disinfection by Hybrid Ag/CS@MnO ₂ Nanosheets Using Near-Infrared Light. ACS Applied Materials & Interfaces, 2019, 11, 15014-15027.	8.0	86
122	Lightâ€Activated Rapid Disinfection by Accelerated Charge Transfer in Red Phosphorus/ZnO Heterointerface. Small Methods, 2019, 3, 1900048.	8.6	64
123	Systemic administration of enzyme-responsive growth factor nanocapsules for promoting bone repair. Biomaterials Science, 2019, 7, 1675-1685.	5.4	31
124	"Imitative―click chemistry to form a sticking xerogel for the portable therapy of bacteria-infected wounds. Biomaterials Science, 2019, 7, 5383-5387.	5.4	17
125	Strontium Promotes the Proliferation and Osteogenic Differentiation of Human Placental Decidual Basalis- and Bone Marrow-Derived MSCs in a Dose-Dependent Manner. Stem Cells International, 2019, 2019, 1-11.	2.5	8
126	Repeatable Photodynamic Therapy with Triggered Signaling Pathways of Fibroblast Cell Proliferation and Differentiation To Promote Bacteria-Accompanied Wound Healing. ACS Nano, 2018, 12, 1747-1759.	14.6	303

#	Article	IF	CITATIONS
127	Defect enhances photocatalytic activity of ultrathin TiO2 (B) nanosheets for hydrogen production by plasma engraving method. Applied Catalysis B: Environmental, 2018, 230, 11-17.	20.2	125
128	Nanosized strontium substituted hydroxyapatite prepared from egg shell for enhanced biological properties. Journal of Biomaterials Applications, 2018, 32, 896-905.	2.4	19
129	Electrophoretic Deposited Stable Chitosan@MoS ₂ Coating with Rapid In Situ Bacteriaâ€Killing Ability under Dual‣ight Irradiation. Small, 2018, 14, e1704347.	10.0	171
130	Nano Ag/ZnO-Incorporated Hydroxyapatite Composite Coatings: Highly Effective Infection Prevention and Excellent Osteointegration. ACS Applied Materials & amp; Interfaces, 2018, 10, 1266-1277.	8.0	127
131	Effects of both Sr and Mg substitution on compositions of biphasic calcium phosphate derived from hydrothermal method. International Journal of Applied Ceramic Technology, 2018, 15, 210-222.	2.1	10
132	Organic composite-mediated surface coating of human acellular bone matrix with strontium. Materials Science and Engineering C, 2018, 84, 12-20.	7.3	22
133	Controlled and sustained drug release performance of calcium sulfate cement porous TiO ₂ microsphere composites. International Journal of Nanomedicine, 2018, Volume 13, 7491-7501.	6.7	10
134	Two-Dimensional Lamellar Mo ₂ C for Electrochemical Hydrogen Production: Insights into the Origin of Hydrogen Evolution Reaction Activity in Acidic and Alkaline Electrolytes. ACS Applied Materials & Interfaces, 2018, 10, 40500-40508.	8.0	38
135	Metal-Free Triple Annulation of Ene–Yne–Ketones with Isocyanides: Domino Access to Furan-Fused Heterocycles via Furoketenimine. Organic Letters, 2018, 20, 6750-6754.	4.6	29
136	Correlation between Mechanical Strength of Amorphous TiO ₂ Nanotubes and Their Solid State Crystallization Pathways. ChemistrySelect, 2018, 3, 10711-10716.	1.5	0
137	Unraveling the osteogenesis of magnesium by the activity of osteoblasts <i>in vitro</i> . Journal of Materials Chemistry B, 2018, 6, 6615-6621.	5.8	38
138	Noninvasive rapid bacteria-killing and acceleration of wound healing through photothermal/photodynamic/copper ion synergistic action of a hybrid hydrogel. Biomaterials Science, 2018, 6, 2110-2121.	5.4	168
139	Controlled-temperature photothermal and oxidative bacteria killing and acceleration of wound healing by polydopamine-assisted Au-hydroxyapatite nanorods. Acta Biomaterialia, 2018, 77, 352-364.	8.3	180
140	The synergistic effect of strontium-substituted hydroxyapatite and microRNA-21 on improving bone remodeling and osseointegration. Biomaterials Science, 2018, 6, 2694-2703.	5.4	39
141	Tuning the Bandgap of Photo-Sensitive Polydopamine/Ag ₃ PO ₄ /Graphene Oxide Coating for Rapid, Noninvasive Disinfection of Implants. ACS Central Science, 2018, 4, 724-738.	11.3	227
142	Rapid Biofilm Eradication on Bone Implants Using Red Phosphorus and Nearâ€Infrared Light. Advanced Materials, 2018, 30, e1801808.	21.0	364
143	DNA nanomachine-based regenerated sensing platform: a novel electrochemiluminescence resonance energy transfer strategy for ultra-high sensitive detection of microRNA from cancer cells. Nanoscale, 2017, 9, 2310-2316.	5.6	77
144	Highly Efficient Electrochemiluminescence Resonance Energy Transfer System in One Nanostructure: Its Application for Ultrasensitive Detection of MicroRNA in Cancer Cells. Analytical Chemistry, 2017, 89, 6029-6035.	6.5	81

#	Article	IF	CITATIONS
145	Four-electron oxygen reduction from mesoporous carbon modified with Fe2O3 nanocrystals. Journal of Materials Science, 2017, 52, 10938-10947.	3.7	16
146	A facile technique for fabricating poly (2-methacryloyloxyethyl phosphorylcholine) coatings on titanium alloys. Journal of Coatings Technology Research, 2017, 14, 1127-1135.	2.5	2
147	Incorporation of silver and strontium in hydroxyapatite coating on titanium surface for enhanced antibacterial and biological properties. Materials Science and Engineering C, 2017, 71, 852-861.	7.3	116
148	Synthesis, Characterization, and Biological Evaluation of Nanostructured Hydroxyapatite with Different Dimensions. Nanomaterials, 2017, 7, 38.	4.1	21
149	The Incorporation of Strontium in a Sodium Alginate Coating on Titanium Surfaces for Improved Biological Properties. BioMed Research International, 2017, 2017, 1-11.	1.9	17
150	Emission Laws and Influence Factors of Greenhouse Gases in Saline-Alkali Paddy Fields. Sustainability, 2016, 8, 163.	3.2	15
151	Effect of freeze–thaw cycles on carbon stocks of saline–alkali paddy soil. Archives of Agronomy and Soil Science, 2016, 62, 1640-1653.	2.6	15
152	Enhancement of gas-sensing abilities in p-type ZnWO4 by local modification of Pt nanoparticles. Analytica Chimica Acta, 2016, 927, 107-116.	5.4	26
153	Nanoporous CuS with excellent photocatalytic property. Scientific Reports, 2016, 5, 18125.	3.3	117
154	Controlled release behaviour and antibacterial effects of antibiotic-loaded titania nanotubes. Materials Science and Engineering C, 2016, 62, 105-112.	7.3	76
155	Synthesis of Cu ₂ O Octadecahedron/TiO ₂ Quantum Dot Heterojunctions with High Visible Light Photocatalytic Activity and High Stability. ACS Applied Materials & Interfaces, 2016, 8, 91-101.	8.0	132
156	Surface Functionalization of Titanium Alloy with miR-29b Nanocapsules To Enhance Bone Regeneration. ACS Applied Materials & Interfaces, 2016, 8, 5783-5793.	8.0	32
157	Synthesis, characterization and biological evaluation of strontium/magnesium-co-substituted hydroxyapatite. Journal of Biomaterials Applications, 2016, 31, 140-151.	2.4	27
158	Strontium incorporation to optimize the antibacterial and biological characteristics of silver-substituted hydroxyapatite coating. Materials Science and Engineering C, 2016, 58, 467-477.	7.3	91
159	New Toxicity Mechanism of Silver Nanoparticles: Promoting Apoptosis and Inhibiting Proliferation. PLoS ONE, 2015, 10, e0122535.	2.5	83
160	Preparation of hydroxyapatite layer on Ti-based bulk metallic glasses by acid and alkali pre-treatment. Rare Metals, 2015, 34, 22-27.	7.1	2
161	Titania nanotube delivery fetal bovine serum for enhancing MC3T3-E1 activity and osteogenic gene expression. Materials Science and Engineering C, 2015, 56, 438-443.	7.3	12
162	Synthesis, characterization and the formation mechanism of magnesium- and strontium-substituted hydroxyapatite. Journal of Materials Chemistry B, 2015, 3, 3738-3746.	5.8	63

#	Article	IF	CITATIONS
163	microRNA-21 promotes osteogenic differentiation of mesenchymal stem cells by the PI3K/β-catenin pathway. Journal of Orthopaedic Research, 2015, 33, 957-964.	2.3	106
164	Pd-loaded In ₂ O ₃ nanowire-like network synthesized using carbon nanotube templates for enhancing NO ₂ sensing performance. RSC Advances, 2015, 5, 30038-30045.	3.6	29
165	Anti-fouling properties of polylactic acid film modified by pegylated phosphorylcholine derivatives. Materials Chemistry and Physics, 2014, 143, 929-938.	4.0	13
166	Fabrication, characterization, and photocatalytic properties of anatase TiO2 nanoplates with exposed {001} facets. Journal of Nanoparticle Research, 2014, 16, 1.	1.9	9
167	Preparation of Nanoporous Pd/CuO by Dealloying and Their Electrocatalysis for Methanol in Alkaline Condition. Journal of the Electrochemical Society, 2014, 161, F1474-F1480.	2.9	13
168	Cytotoxicity and antibacterial property of titanium alloy coated with silver nanoparticle-containing polyelectrolyte multilayer. Materials Science and Engineering C, 2013, 33, 2816-2820.	7.3	44
169	Fabrication of dopamine-modified hyaluronic acid/chitosan multilayers on titanium alloy by layer-by-layer self-assembly for promoting osteoblast growth. Applied Surface Science, 2013, 284, 732-737.	6.1	51
170	Effect of gas nitriding treatment on cavitation erosion behavior of commercially pure Ti and Tiâ^'6Alâ^'4V alloy. Surface and Coatings Technology, 2013, 221, 29-36.	4.8	36
171	Preclinical evaluation of strontium-containing bioactive bone cement. Materials Science and Engineering C, 2013, 33, 5100-5104.	7.3	6
172	Variation of Soil Organic Carbon Stock under Land Use and Land Cover Changes in Farming-Pastoral Ecotone over the Past Century in Zhenlai, China. , 2012, , .		1
173	The cross-talk between osteoclasts and osteoblasts in response to strontium treatment: Involvement of osteoprotegerin. Bone, 2011, 49, 1290-1298.	2.9	118
174	Osteoprotegerin deficiency attenuates strontium-mediated inhibition of osteoclastogenesis and bone resorption. Journal of Bone and Mineral Research, 2011, 26, 1272-1282.	2.8	50
175	Strontium Promotes Osteogenic Differentiation of Mesenchymal Stem Cells Through the Ras/MAPK Signaling Pathway. Cellular Physiology and Biochemistry, 2009, 23, 165-174.	1.6	245
176	Strontium–calcium coadministration stimulates bone matrix osteogenic factor expression and new bone formation in a large animal model. Journal of Orthopaedic Research, 2009, 27, 758-762.	2.3	35
177	Vertebral Augmentation With a Novel Vessel-X Bone Void Filling Container System and Bioactive Bone Cement. Spine, 2007, 32, 2076-2082.	2.0	24
178	Study on the curing process of QY8911-3 resin. Journal of Applied Polymer Science, 2003, 89, 3769-3773.	2.6	0